

Absence of *Chx10* Causes Neural Progenitors to Persist in the Adult Retina

Nathalie S. Dhomen,¹ Kam S. Balaggan,² Rachael A. Pearson,¹ James W. Bainbridge,² Edward M. Levine,³ Robin R. Ali,² and Jane C. Sowden¹

PURPOSE. Mutation of the *Chx10* homeobox gene in mice and humans causes congenital blindness and microphthalmia (small eyes). This study used *Chx10*^{-/-} (ocular retardation) mice to investigate how lack of Chx10 affects progenitor/stem cell behavior in the retina and ciliary epithelium (CE).

METHODS. The distribution of mitotic retinal progenitor cells (RPCs) during embryonic development was analyzed using phosphohistone 3 (H3)-labeling. DNA flow cytometry was used to measure DNA content. The distribution and phenotype of dividing cells in the postnatal retina and CE was analyzed by incorporation of the thymidine analogue BrdU and immunohistochemistry.

RESULTS. The *Chx10*^{-/-} embryonic retina maintained a constantly sized population of mitotic RPCs during development, causing the mitotic index to increase markedly over time compared with the wild type. Also, the proportion of cells in the G₁ phase of the cell cycle was increased compared with the wild type. Of interest, division of RPC-like cells with neurogenic properties persisted in the adult *Chx10*^{-/-} retina. Colabeling for BrdU and the neural progenitor marker nestin or the neuronal markers β 3-tubulin, syntaxin, and VC1.1 showed that new amacrine-like neurons developed in the adult central retina. By contrast, cells with these characteristics were not observed in the mature wild-type retina. In the mature CE, BrdU-positive cells were observed in both wild-type and *Chx10*^{-/-} mice. However, neurogenesis from this cell population was not evident.

CONCLUSIONS. Without *Chx10*, proliferative expansion of the embryonic RPC pool is markedly reduced. In the adult retina, lack of *Chx10* results in a population of dividing neural progenitor cells that persist and produce new neurons in the

central retina. (*Invest Ophthalmol Vis Sci.* 2006;47:386-396)
DOI:10.1167/iovs.05-0428

Organ size is determined largely by cell number, as well as by cell size.¹ How many cells an organ contains is laid down in development and involves a sequence of progenitor cell divisions, usually ending in a full complement of postmitosis differentiated cells. The continued presence of dividing undifferentiated cells in adult tissues, termed stem cells, which maintain and repair tissue by generating new specialized cells is well characterized in, for example, the intestinal epithelium.^{2,3} Although most regions of the mature central nervous system are considered unable to generate new neurons once neurogenesis during development is complete, some neurogenesis occurs within specific stem cell-containing regions.⁴ Characterization of neural stem cells is offering new insights into regenerative potential in mammals.^{5,6} However, little is known about the relationship between progenitor/stem cells in embryonic and adult life and how developmental conditions influence their behavior.

The neural retina (NR) is an ideal system for studying how part of the nervous system achieves its adult size by regulation of neural progenitor/stem cells. The NR forms from evaginations of the anterior neural plate, which form the bilayered optic cup at embryonic day (E)10.5 in the mouse. The inner layer of the cup, the presumptive NR, comprises multipotential retinal progenitor cells (RPCs). Retinal volume, which consequently affects eye size, is primarily determined by the number of divisions that each progenitor cell makes before its final division to generate two postmitotic cells. By the time retinal histogenesis is complete at approximately postnatal day (P)11, there are no more proliferating RPCs.^{7,8} During this period of histogenesis (E10.5-P11), the large increase in eye size results directly from the proliferative expansion of the RPCs.

Overexpression of several eye-specific transcription factors results in giant eyes.^{9,10} Lack of other transcription factors, as well as mutations in cell cycle proteins, reduce eye size.¹¹⁻¹³ Reduced eye size in humans is the condition called microphthalmia and is a cause of congenital blindness. Mutations in several different genes have been shown to cause microphthalmia, indicating the genetic heterogeneity of this condition (reviewed in Ref. 14). Mutation of the human *CHX10* gene and the mouse *Chx10* gene causes microphthalmia.¹⁵⁻¹⁷ The *Chx10* mutant, ocular retardation, lacks bipolar cells, and differentiation of rod photoreceptors is disrupted.^{16,18} *Chx10* is an early marker of NR and is expressed in RPCs throughout development.^{19,20} Chx10 is essential for RPC proliferation and lack of proliferation in the *Chx10* mutant is partially rescued by deletion of the cell cycle regulatory gene p27(Kip1).^{16,21-23} DNA synthesis in the *Chx10* mutant has been examined by quantifying incorporation of the thymidine analogue, bromodeoxyuridine (BrdU). A large reduction in BrdU labeling was found at the periphery of the embryonic retina, but labeling indices were not significantly altered in the central retina.^{16,24}

The ciliary epithelium (CE) of the ciliary body, at the periphery of the adult mammalian retina, has recently been

From the ¹Developmental Biology Unit, Institute of Child Health, and the ²Institute of Ophthalmology, University College of London, London, United Kingdom; and the ³John A. Moran Eye Center, University of Utah, Salt Lake City, Utah.

Supported in part by a Medical Research Council Grant 67396 (RRA, JCS) and in part by Grant EY013760 from the National Eye Institute (EML), the Foundation Fighting Blindness (EML), and a career development award from Research to Prevent Blindness (EML). Research at the Institute of Child Health and Great Ormond Street Hospital for Children National Health Service (NHS) Trust benefits from research and development funding received from the NHS Executive. NSD is a Research Student supported by Fight for Sight, United Kingdom.

Submitted for publication April 5, 2005; revised August 9 and October 6, 2005; accepted November 23, 2005.

Disclosure: N.S. Dhomen, None; K.S. Balaggan, None; R.A. Pearson, None; J.W. Bainbridge, None; E.M. Levine, None; R.R. Ali, None; J.C. Sowden, None

The publication costs of this article were defrayed in part by page charge payment. This article must therefore be marked "advertisement" in accordance with 18 U.S.C. §1734 solely to indicate this fact.

Corresponding author: Jane C. Sowden, Developmental Biology Unit, Institute of Child Health, UCL, 30 Guilford Street, London WC1N 1EH, UK; j.sowden@ich.ucl.ac.uk.

shown to harbor cells with stem cell properties of multipotentiality and self-renewal in vitro.^{25,26} The CE develops from the neuroepithelium at the periphery of the embryonic optic cup. Adult CE-derived stem cells (in neurosphere cultures) express *Chx10* and the neural progenitor/stem cell marker nestin and, when differentiated, express retinal neuron specific markers.²⁵ Notably, more neurospheres arose from the CE of the *Chx10*-null mouse than from wild-type cultures.²⁶ In nonmammalian vertebrates the peripheral zone of the retina is referred to as the ciliary marginal zone and contains stem cells that generate new neurons for retinal growth throughout life.²⁷

In this study, we used *Chx10*-null mice to investigate how lack of *Chx10* affects progenitor/stem cell behavior in the retina and CE in vivo. We found that in the absence of *Chx10*, proliferative expansion of embryonic RPCs was markedly reduced. Of interest, we also found a novel population of RPC-like cells with neurogenic potential in the mature *Chx10*-null retina.

METHODS

H3 and TUNEL Immunohistochemistry of Wild-Type and *Chx10* Mutant Mouse Eyes

All animal procedures were performed in accordance with the ARVO Statement for the Use of Animals in Ophthalmic and Vision Research. Timed matings of ocular retardation mice with the *Chx10^{orj/orj}* mutation (referred to as *Chx10^{-/-}*) on a pigmented 129/Sv genetic background and 129/Sv wild-type mice (+/+) were performed to produce embryos at various stages of development. Days on which plugs were found after overnight matings were considered to be embryonic day (E)0.5. Wild-type and mutant embryos at E11.5, E13.5, E15.5, and E18.5 were fixed in 4% paraformaldehyde in phosphate-buffered saline (PBS) overnight and subsequently transferred to 20% sucrose in PBS for overnight incubation. The tissue was embedded in optimal cutting temperature (OCT) compound, and 7- μ m-thick retinal cryosections were prepared on 3-aminopropyltriethoxysilane (TESPA; Sigma-Aldrich, Poole, UK)-coated slides. Sections were dried at room temperature overnight and stored at -80°C before use.

Mitotic RPCs were identified by anti-phosphohistone H3 immunohistochemistry. The H3 antibody detects phosphorylation at Ser10 of histone H3 which is at high levels during chromosome condensation at entry into the M-phase.²⁸ RPCs are located at the ventricular surface adjacent to the RPE during the M-phase.²⁹ For immunostaining, sections were incubated in blocking solution (10% fetal calf serum, FCS, 1% bovine serum albumin, BSA, and 0.1% Tween 20 in PBS) for 1 hour, and then incubated with primary antibody, rabbit anti-phosphohistone 3 (H3, 1:100 dilution in blocking solution; Upstate Biotechnology, Lake Placid, NY), overnight at 4°C . Sections were incubated with FITC-conjugated anti-rabbit antibody (1:100 in blocking solution; Jackson ImmunoResearch, Inc., West Grove, PA) and Hoechst nuclear dye (1:1000), for 1 hour before mounting. The total number of retinal cells (Hoechst-stained) and the number of mitotic cells (H3-labeled) were counted on nine midline retinal sections from three eyes from mutant and wild-type animals at all time points (E11.5, E13.5, E15.5, and E18.5). An H3 labeling index was obtained by dividing the number of H3-labeled cells by the total number of cells in each section. Two-way analysis of variance was performed on computer (SPSS ver. 11; SPSS, Chicago, IL), to check for interaction between mutant and wild-type mice and the various time points. To correct for the higher chance of making false-positive conclusions from the multiple pair-wise comparisons, after an interaction was found, we further analyzed the significant simple main effects by pair-wise comparisons using the Sidak adjustment for multiple comparisons. $P < 0.05$ was considered significant.³⁰

The terminal deoxynucleotidyl transferase (TdT)-mediated deoxyuridine triphosphate (dUTP)-biotinylated nick-end labeling (TUNEL) assay was performed to identify apoptotic cells in embryonic

retinal sections (In Situ Cell Death Detection Kit; Roche Diagnostics, Mannheim, Germany),³¹ according to the manufacturer's protocol. The TUNEL kit detected apoptotic cells within the retina and other control tissues (e.g., embryonic brain).

Cell Cycle Analysis with DNA Content Flow Cytometry

DNA content flow cytometry^{32,33} was used to analyze embryonic RPCs. NR tissue from E11.5 *Chx10^{-/-}* mutant and wild-type embryos was microdissected with tungsten watchmaker forceps in cold PBS. Retinal tissue was treated with 0.05% trypsin and 0.53 mM EDTA for 10 minutes at 37°C and then quenched with fetal calf serum. Tissue was triturated gently to form a single-cell suspension. Cells were centrifuged at $14,000g$ for 1 minute, washed with PBS and counted on a hemocytometer, before resuspension in 70% ethanol for storage at 4°C (for 1-14 days) until analysis. Cells were resuspended in 50 $\mu\text{g}/\text{mL}$ propidium iodide, 0.1% wt/vol sodium citrate, 0.1% Triton X-100 vol/vol. The samples, containing 5×10^5 to 1×10^6 cells, were immediately run on a flow cytometer (Epics XL; Beckman Coulter, Fullerton, CA). In total, 30,000 events were collected and gated using doublet discrimination to exclude clumps of cells. Expo32 (Beckman Coulter) was used to select only single cells in the cell cycle (i.e., excluding dead or fragmented cells), and the data were subsequently modeled (Multicycle; Phoenix Flow Systems, San Diego, CA). The data fitted the aggregate model used for analysis of single cells. Graphs were obtained (Multicycle; Phoenix Flow Systems) to determine the proportion of the total cells in the different phases of the cell cycle—the G_1 peak, S-phase, or G_2 peak, based on the level of propidium iodide labeling (i.e., G_2 cells contained twice as much propidium iodide as G_1 cells). Triplicate flow cytometry experiments were performed on retina dissected from six litters ($n = 4$ to 7 embryos per experiment). Mean average cell percentages \pm SD in each stage of the cell cycle were calculated. Student's *t*-test was used to test for significant differences between mutant *Chx10^{-/-}* and wild type at the G_1 , G_2 , and S stages of the cell cycle.

BrdU Labeling and Immunohistochemistry of Wild-Type and *Chx10* Mutant Mouse Eyes

Incorporation of the thymidine analogue BrdU into newly synthesized DNA during the S-phase was used as an assay for cell proliferation. Immunostaining for incorporated BrdU allowed identification of cells that divided after the first BrdU injection. Wild-type and mutant *Chx10^{-/-}* mice were given an intraperitoneal injection of BrdU (Sigma-Aldrich) diluted at 10 mg/mL in 0.1 M Tris (pH 7), at 100 $\mu\text{g}/\text{g}$ body weight at 2 (P14), 3 (P21), and 6 (P42) weeks of age. The mice were subsequently injected every other day for 2 weeks after the first injection, and tissue was prepared on the day after the last injection. This protocol identified cells that divided during the 2-week period of injections. For single developmental time points, animals were injected, for example, on P7, and the tissue was prepared 24 hours later, on P8. For experiments to immunolabel neuronal subtypes, mice were injected at P25, P27, and P29, and tissue was prepared 3 weeks after the last injection. The 3-week chase period allowed time for cells that had incorporated BrdU to differentiate. Animals were given a terminal anesthetic (0.2 mL of 200 mg/mL pentobarbital sodium for adult mice) and perfused with saline to remove blood, before the eyes were dissected and fixed in Carnoy's fixative: 60% ethanol, 30% chloroform, 10% acetic acid, for 15 minutes. Alternatively, animals were perfused with 4% paraformaldehyde rather than saline, and required no further fixing. Eyes were embedded in paraffin wax and cut into 7- μ m sections.

For BrdU immunostaining, tissue sections were dewaxed for 10 minutes (Histoclear; Raymond H. Lamb, Eastbourne, UK) and rehydrated through graded concentrations of ethanol, followed by incubation in distilled water for 5 minutes. The slides were heated in a microwave at 540 W in 0.01 M citric acid (pH 6.0) for 6 minutes and cooled in circulating water for 10 minutes before being rinsed twice in

PBS. The sections were incubated in 0.1 M HCl for 30 minutes at room temperature and then in 2 M HCl for 30 minutes at 37°C, followed by a 10-minute incubation in sodium borate (pH 8.5) at room temperature. Nonspecific binding sites were blocked with 10% FCS and 1% BSA for 1 hour at room temperature, followed by incubation with rat anti-BrdU antibody (1:100; Immunologicals Direct, Oxfordshire, UK) at 4°C overnight. Slides were then incubated with FITC-conjugated anti-rat secondary antibody (1:100; Insight Biotechnology, Wembley, UK) for 40 minutes before mounting.

For statistical analysis, BrdU-labeled cells were counted on midline retinal sections from three to seven eyes from mutant and wild-type animals at 4 and 8 weeks of age (after BrdU injection every other day for 2 weeks). Student's *t*-tests were performed on differences between mutant and wild-type counts at the two time points to determine significance ($P < 0.05$).

To identify types of proliferating cells in the adult retina, double-labeling experiments were performed using the stem-progenitor marker nestin and the two pan-neuronal markers NeuN and β 3-tubulin (Tuj1). Brn3b (Pou4f2) was selected as a marker for ganglion cells, blue cone opsin for cones, rhodopsin for rods, recoverin for both rod and cone photoreceptors, syntaxin and the VC1.1 epitope for amacrine and horizontal cells, glial fibrillary protein (GFAP) for Müller cells, and cellular retinaldehyde-binding protein (CRALBP) for Müller glial cells and retinal pigmented epithelium (RPE).^{18,34,35} β 1-Integrin was used as an endothelial cell marker. For double labeling of BrdU and nestin, β 3-tubulin, NeuN, β 1-integrin, Brn3b (Pou4f2), rhodopsin, blue cone opsin, GFAP, protein kinase C (PKC), syntaxin, or VC1.1, the sections were treated as just described, but after the blocking step, they were incubated with mouse anti-nestin antibody (1:10; Developmental Studies Hybridoma Bank, Iowa City, IA), anti- β 3-tubulin (1:1000; Promega, Madison, WI), anti- β 1-integrin (1:100; Transduction Laboratories, Lexington, KY), anti-NeuN (1:50; Chemicon, Torrance, CA), anti-PKC (1:100; Sigma-Aldrich); anti-syntaxin (1:100; Sigma-Aldrich) or anti-VC1.1 (HNK-1) antibody (1:100; Sigma-Aldrich); goat anti-Brn3b (1:100; Santa Cruz) or anti-rhodopsin antibody (1:50; Santa Cruz); or chicken anti-blue cone opsin antibody³⁶ (1:5000) or rabbit anti-GFAP antibody (1:100; Dako, High Wycombe, UK) at 4°C overnight. Incubation with primary antibody was followed by a 1-hour incubation with the appropriate species-specific secondary antibody: Cy3-conjugated anti-mouse antibody (1:100; Jackson ImmunoResearch), Cy3-conjugated anti-goat antibody (1:100; Jackson ImmunoResearch), Alexa-594-conjugated anti-chicken antibody (1:100; Molecular Probes, Eugene, OR), or rhodamine-conjugated anti-rabbit antibody (1:100; Jackson ImmunoResearch). Rabbit anti-recoverin antibody (1:100; Chemicon) and rabbit anti-CRALBP antibody (1:1000; kindly provided by Jack Saari, Department of Biochemistry, University of Washington, Seattle, WA) were used, together with a TRITC-conjugated anti-rabbit antibody (1:100; Jackson ImmunoResearch). After the slides were washed in PBS, they were then incubated with anti-BrdU antibody (1:100) for 2 hours, followed by incubation in secondary antibody for 40 minutes.

To immunolabel subtypes of dissociated retinal cells, *Cbx10*^{-/-} mutant ($n = 5$) and wild-type ($n = 5$) mice were injected with BrdU at P25, P27, and P29, and tissue was prepared 3 weeks after the first injection. NRs were dissected in DMEM and dissociated with a papain-based cell-dissociation system (Worthington Biochemicals, Freehold, NJ). The cells were resuspended in Tris-buffered saline (TBS), plated on poly-L-lysine-coated slides, and air dried for 20 minutes before being fixed for 10 minutes with 4% paraformaldehyde. The slides were washed and treated with 2 M HCl for 20 minutes and 0.1 M sodium borate for 10 minutes and incubated with blocking solution (10% normal goat serum, 1% BSA in TBS) for 30 minutes. Immunohistochemistry for BrdU and the neuronal markers was performed sequentially. Each primary antibody was applied for 1 hour, slides were washed three times for 2 minutes each in TBS, and the appropriate secondary antibody was applied for 30 minutes. After incubation with the final secondary, slides were washed three times for 5 minutes each in TBS, and the nucleic marker Hoechst 33342 (2 μ M) was included in the final wash.

All slides were mounted with glycerol/PBS solution (Citifluor; Agar Scientific, Stansted, UK). Slides were viewed using one of two confocal microscopes (Axioptot2; Carl Zeiss Meditec, Inc., Dublin, CA; or Leica, Deerfield, IL) and digital images captured (Openlab; Improvision, Heidelberg, Germany, or Leica Confocal Software; transferred to Photoshop; Adobe Systems, Mountain View, CA).

RESULTS

Influence of Mitosis in the *Cbx10*^{-/-} Mutant Retina on the Size of the RPC Population

Studies measuring BrdU incorporation have shown that in the absence of Chx10, very few RPCs in the peripheral retina at the outer edge of the optic cup synthesize DNA. However in the central retina BrdU labeling indices were not significantly different between wild-type and *Cbx10*^{-/-}.^{16,24} To examine further the cycling behavior of Chx10-expressing RPCs in the central retina, we compared changes in the number of M-phase cells during development. We used anti-phosphohistone H3 immunohistochemistry, which strongly labels cells during metaphase,²⁸ to compare the distribution of mitotic cells in the wild-type eye and in the *Cbx10*-null mutant mouse, during embryonic development (Fig. 1). H3-positive mitotic cells located at the ventricular edge of the proliferating cell layer were detected in the wild-type and mutant retina at E11.5 to E18.5. From E13.5 onward a lack of H3 labeling was observed in the periphery of the mutant retina (Fig. 1D), which is consistent with previous reports of reduced BrdU incorporation at the periphery.^{16,24} By contrast, H3-positive cells were detected in the central retina of mutant and wild-type throughout embryogenesis. Immunostaining with PCNA (proliferating cell nuclear antigen) which labels progenitors throughout the cell cycle, confirmed the pattern of reduced proliferation at the retinal periphery compared with central retina (data not shown). At E15.5 and E18.5, abnormal positioning of mitotic cells was occasionally observed in the mutant (Figs. 1G, 1H).

In the *Cbx10*^{-/-} embryonic retina, expansion of the total cell number and the mitotic cell number failed to keep up with the wild-type retina (Figs. 2A, 2B). From E13.5 onward, both the total number of cells and the number of H3-labeled mitotic cells were significantly reduced in the mutant compared with the wild type (Figs. 2A, 2B).

To compare the number of mitotic cells in mutant and wild-type retina, we estimated the mitotic labeling index at each stage from midline retinal sections (Fig. 2A–C). At E11.5, a similar proportion of the total cells in the wild-type and mutant were undergoing mitosis (Fig. 2C). In both the mutant and the wild type, the mitotic index decreased significantly from E11.5 to E13.5 (Fig. 2C). Of note, from E15.5 onward the mitotic index is significantly higher in the mutant compared with the wild-type retina.

From E13.5 to E18.5, the wild-type pattern of growth (increasing total number of cells) causes a significantly decreasing mitotic index (Fig. 2C). By contrast, no significant change was observed in the mitotic index from E13.5 to E18.5 in the mutant retina (Fig. 2C). Whereas the absolute number of H3-labeled cells significantly increased during the embryonic period (E11.5–E18.5) in the wild-type retina, the number was constant in the mutant, over the same period (Fig. 2B). A large expansion in the size of the pool of dividing RPCs was not observed in the mutant, despite the presence of mitotic cells throughout embryogenesis in a proportion similar to the number of mitotic cells present at E11.5 in the wild type (compare E18.5 mutant with E11.5 wild type in Fig. 2B).

We next used DNA flow cytometry to measure the DNA content of dissociated RPCs and compare the percentage of

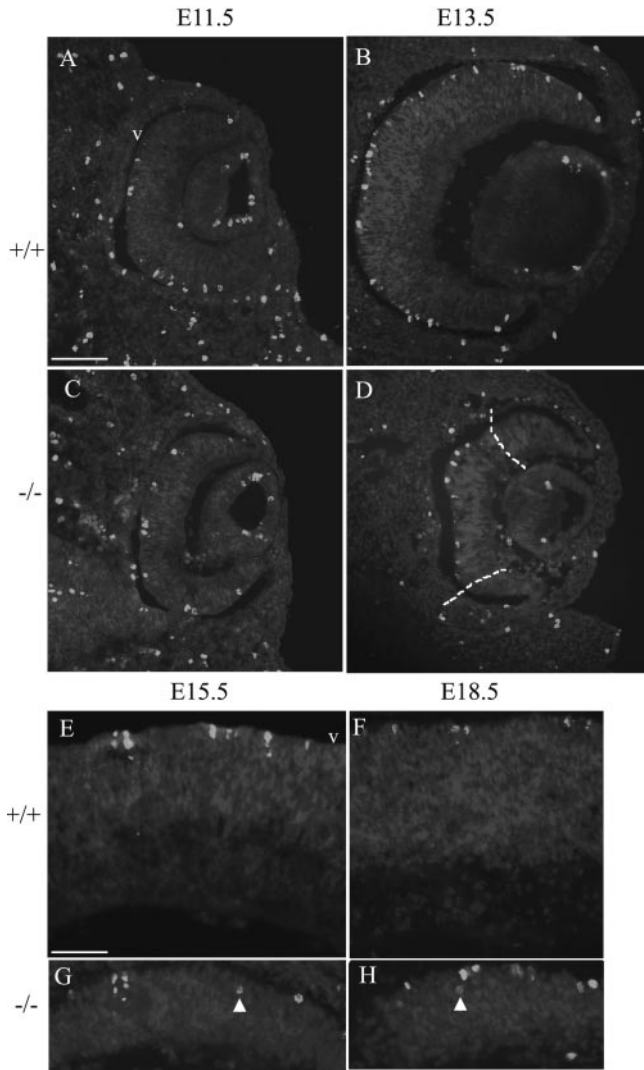


FIGURE 1. H3-labeled cells in the developing retina. Midline sections from wild-type (+/+, A, B, E, F) and mutant (-/-, C, D, G, H) eyes at E11.5, E13.5, E15.5, and E18.5, labeled with H3 antibody (white) and counterstained with Hoechst nuclear dye. At E11.5 (A, C), wild-type and mutant retina showed a similar number of mitotic H3-positive cells along the ventricular surface (v). At E13.5 (B, D), the wild-type retina was larger than the mutant. More cells were labeled in the wild-type retina than in the mutant retina, and no cells were labeled in the periphery of the mutant retina (dashed white lines demarcating the central retina in D). (E-H) show mitotic cells in the E15.5 (E, G) and E18.5 (F, H) mutant and wild-type central retinae. H3-positive cells displaced from the ventricular surface (v) were present in the mutant retina at E15.5 and E18.5 (arrowheads). Scale bars: (A-D) 100 μ m; (E-H) 50 μ m.

cells at the G₁, G₂, and S stages of the cell cycle in the wild type and mutant. NR from E11.5 wild-type and mutant embryos were dissociated, labeled with propidium iodide and passed through a flow cytometer. The proportion of cells in the G₁, G₂, and S phases were quantified. Of the total cells assayed, 51.4% \pm 1.8% of were in G₁ in the wild type compared with 60.3% \pm 0.5% in the mutant, 38.6% \pm 1.4% were in the S-phase in the wild type compared with 26.5% \pm 1.7% in the mutant, and 10.0% \pm 3.2% were in the G₂-phase in the wild type compared with 13.2% \pm 1.8% in the mutant. These data showed that a higher proportion of cells were in G1 in the mutant than wild type (Fig. 3). Conversely, a decreased number of RPCs were in the S-phase in the mutant retina than in the

wild type. Thus, at the stage when the retinas are largely undifferentiated and similar in size between the mutant and the wild type, the cycling properties of the RPCs differed considerably.

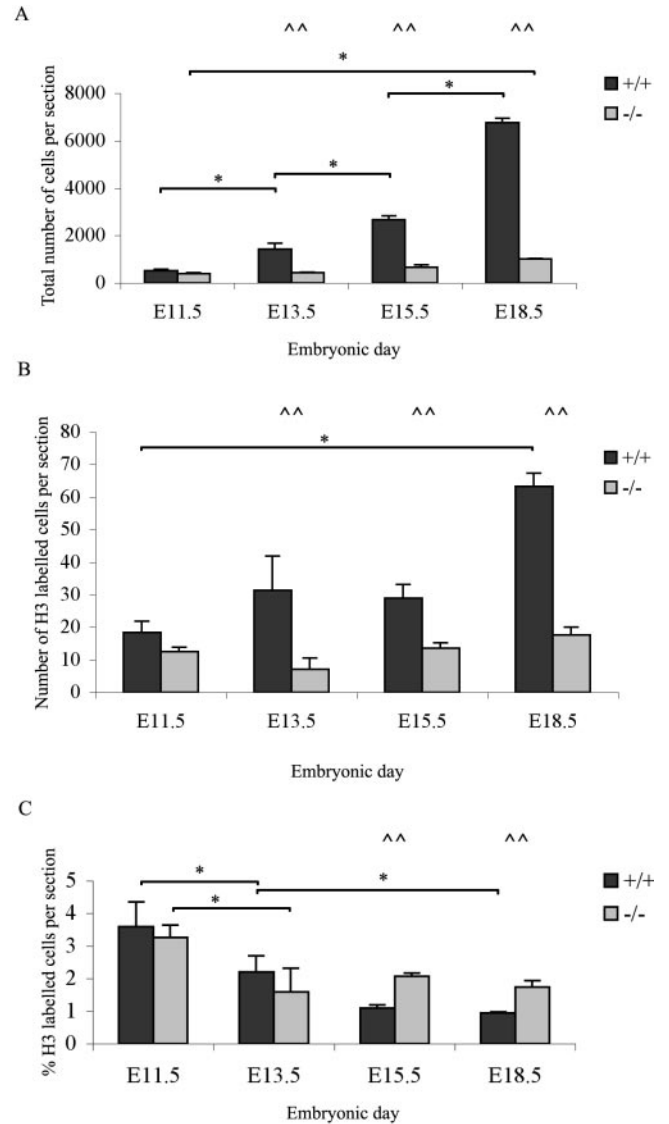


FIGURE 2. Comparison of total number of cells and H3-labeled cells in wild-type and mutant retina. (A) The total number of cells of wild-type retina increased steadily in the wild-type retina during development. Significant increases in total cell number were observed between every time point in the wild type. In the mutant, a small but significant overall increase was observed only between E11.5 and E18.5 (**P* < 0.001). ^^Significant differences between genotypes (*P* < 0.001) at each time point. (B) The number of H3-labeled mitotic cells in the wild-type retina increased significantly between E11.5 and E18.5 (**P* < 0.001). In the mutant, no overall significant increase was observed in H3-labeled cells between E11.5 and E18.5. ^^Significant differences between genotypes (*P* < 0.001). (C) Mitotic labeling index (number of H3-labeled cells divided by the total number of cells, per section). At E11.5, a similar proportion of cells were undergoing mitosis in the mutant and wild-type retina. By E13.5 the mitotic index of both the mutant and wild-type retina had decreased significantly (**P* < 0.01). This trend continued in the wild-type retina throughout development, with a significant difference in mitotic labeling index between E13.5 and E18.5 (**P* < 0.01), but no significant change was observed in the mitotic labeling index from E13.5 onward in the mutant retina. ^^Significant differences between genotypes at each time point (*P* < 0.05). (A-C) data are the mean; error bars, SD) *n* = 9 midline sections taken from three eyes for each condition.

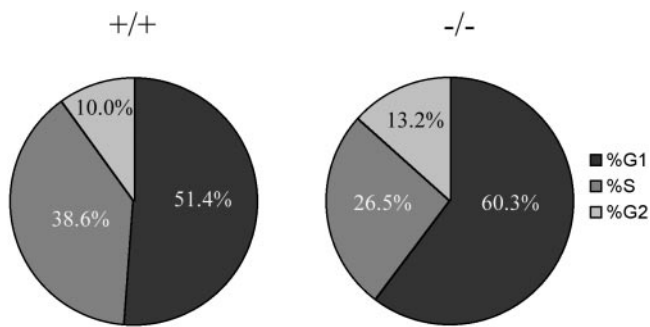


FIGURE 3. Altered properties of *Chx10*^{-/-} retinal progenitors. Pie charts representing the percentage of cells in G₁, G₂, and S stages of the cell cycle in E11.5 wild-type (+/+) and mutant (-/-) retinas as measured by DNA flow cytometry. A significant increase in the percentage of cells in the G₁ phase was observed in the mutant retina compared with the wild type ($P = 0.001$), whereas a significant decrease in the percentage of cells in the S-phase was observed in the mutant ($P = 0.001$). No significant difference was observed in cells in the G₂ phase.

Role of Apoptosis in the Deficit of Cells in the Early Embryonic *Chx10*^{-/-} Retina

TUNEL labeling was used to assess whether increased levels of apoptosis occur during development of the *Chx10*^{-/-} retina, which could explain the low level of retinal growth. Between E11.5 and E18.5, the total number of cells increased 13 times in the wild type compared with 4 times in the mutant (Fig. 2A). Very few apoptotic cells were observed in either the mutant or wild-type retina during embryonic development. No significant difference (Student's *t*-test) was observed between the number of apoptotic cells at E11.5 in the wild-type or mutant retina. Apoptotic cells (9.8 ± 5.0) were observed per midline retinal section in the wild-type retina ($n = 7$ sections, from four embryos), compared with 3.4 ± 2.2 in the mutant retina ($n = 17$ sections, from two embryos). The apparent trend of more apoptosis occurring in the wild type than the mutant is contrary to what would be expected if apoptosis accounted for the deficit

in the number of cells in the *Chx10* mutant. Apoptotic cells were mainly located in the ventral retina around the optic fissure.

Persistence of Proliferation of Cells in the *Chx10*^{-/-} Central Retina in Adulthood

Our findings suggest that in the embryo, *Chx10* plays an important role in the production of rapidly dividing RPCs that are responsible for the expansion in the number of retinal cells. Next, we analyzed the profile of dividing cells in the postnatal and adult retina. Previous birth-dating studies have indicated that retinal histogenesis is normally completed by the end of the second postnatal week (around P11).^{7,37} We used a schedule of repeated BrdU injections that allowed us to observe slowly dividing cells or cells that divide infrequently in the postnatal and adult retina. Wild-type and mutant mice were given intraperitoneal injections every other day from P15 to P29.

As expected, little or no BrdU staining was observed in the central or peripheral wild-type retina (Figs. 4C, 4D, 5A). Of the 28 sections analyzed (seven eyes, four sections each), an average of zero to two labeled cells were found per retinal section. These labeled cells were predominantly located within the inner layers of the retina (Fig. 4D) and were likely to be endothelial in origin (discussed later). Several labeled cells were also observed in the ciliary body, in both the pigmented and nonpigmented CE, although predominantly in the nonpigmented CE (Fig. 4E).

The mutant retina, however, showed a remarkable contrast. A relatively large number of cells were labeled throughout the central retina (Figs. 4A, 5A). This number was substantially higher ($P = 1.75 \times 10^{-5}$) than the occasional labeled cell observed in the wild-type retina (Fig. 5). Labeled cells were also detected in the mutant CE, which is enlarged and disorganized compared with the wild type (Figs. 4B, 5B). A higher number of cells were labeled in the mutant CE than in the wild type (Fig. 5B; $P = 0.01$).

To examine whether proliferation in the mutant retina continues further into adulthood, a follow-up set of injections was performed between 6 to 8 weeks after birth. In the wild-type

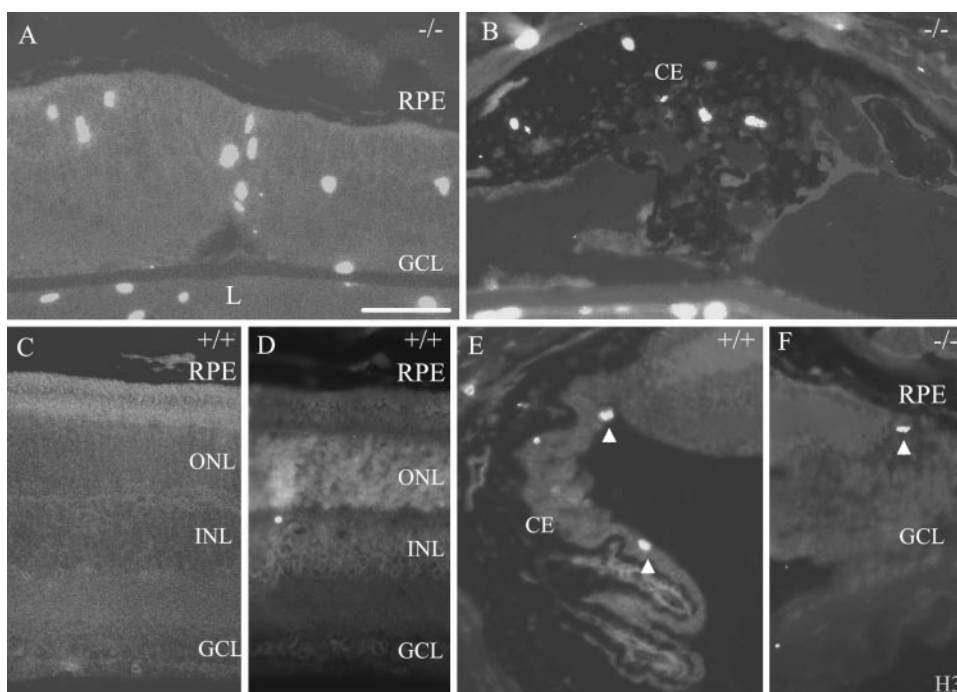


FIGURE 4. Proliferating cells persisted in the adult mutant retina. Sections of mutant (-/-, A, B) and wild-type (+/+, C-E) retina, taken from mice injected with BrdU between P15 and P29, labeled with anti-BrdU antibody (white), and counterstained with Hoechst nuclear dye. In the mutant, many cells were labeled throughout the central retina (A), indicating that proliferation occurred between P15 and P29. The expanded CE of the mutant retina (B) also contained labeled cells. Very few cells were labeled in the wild-type retina (C), and any labeled cells tended to be located around the inner nuclear layer (D). A small number of cells were labeled in the wild-type CE—in most cases, nonpigmented cells (E, arrowheads). (F) H3-positive mitotic cell (arrowhead) in a retinal section from a P20 mutant. ONL, outer nuclear layer; INL, inner nuclear layer; GCL, ganglion cell layer; L, lens; RPE, retinal pigmented epithelium. Scale bar, 50 μ m.

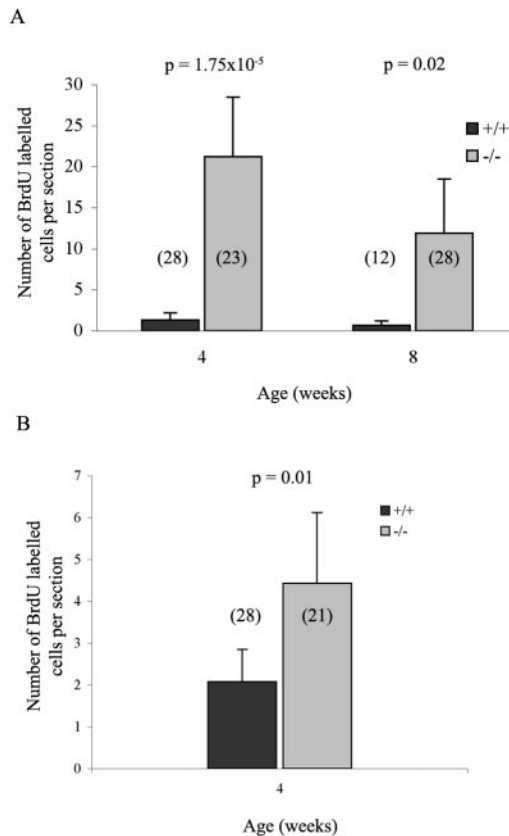


FIGURE 5. More BrdU-labeled cells were present in the mutant compared with wild-type retina. Mice were injected with BrdU for 2 weeks before culling at 4 or 8 weeks, and labeled cells were counted in midline retinal sections and compared. The number of BrdU-labeled cells in the mutant and wild-type retina at 4 and 8 weeks (A), and in the CE at 4 weeks (B). At 4 weeks, less than five cells per section were labeled in the wild-type retina, whereas more than 20 cells per section were labeled in the mutant retina on average. By 8 weeks, very few BrdU-labeled cells were observed in the wild-type retina, whereas a significantly higher average of 12 labeled cells per section was observed in the mutant retina (A). A small but significant difference between the number of labeled cells in the CE of the wild-type and mutant retinas was observed in sections from 4-week-old mice (B). Data are the mean; error bars, SD. Numbers in brackets denote the number of sections examined. At 4 weeks, sections were taken from seven wild-type and six mutant mouse eyes; at 8 weeks, sections were taken from three wild-type and seven mutant mouse eyes.

retina, few or no dividing cells were detected (Fig. 5A). In the mutant retina, a significantly larger number of cells ($P = 0.02$) divide during this 2-week period (Fig. 5A). Although fewer cells were labeled than at 2 to 4 weeks of age, these data indicate that a population of cells in the retina continues to proliferate well into adulthood. H3 immunostaining was also performed on a series of postnatal retinal sections. Whereas H3-positive mitotic cells were not detected at P20 in the wild-type retina, occasional H3-positive cells were seen in the mutant at the ventricular surface in the central retina (Fig. 4F). This study identified a unique feature of the pattern of proliferation in the mutant retina that is very different from that of the wild-type retina.

Fate of BrdU-Labeled Cells in the Adult *Chx10*^{-/-} Mutant Retina

To examine the phenotype of the dividing BrdU-labeled cells we double labeled the BrdU treated eyes with nestin, a marker for neural progenitor/stem cells.^{25,38,39}

In the early postnatal wild-type retina we detected nestin staining of RPCs. Typically nestin-labeled progenitors project radially across the retina laminar axis.⁴⁰ Figures 6A–C show BrdU-labeled cells in wild-type P8 mice (BrdU injected at P7 and mice culled at P8). Colabeling with nestin was observed in RPCs at the periphery of the retina, the last area of the retina to mature and cease proliferation (Figs. 6A, 6B) but not in the central retina, which was largely postmitotic (Fig. 6C). By 4 weeks of age in the wild type, no nestin labeling of RPCs was observed (Fig. 6D). By contrast, nestin labeling was maintained in the mutant in RPC-like cells projecting radially across the retina (Figs. 6E, 6F). Colocalization of BrdU and nestin was detected in a small proportion of cells (Fig. 6F). TUNEL labeling of the postnatal week 4 and 8 retinas did not detect apoptotic cells in the mutant (data not shown), suggesting that cell death was not a common fate. As not all BrdU-labeled cells were labeled with nestin, it seemed likely that these cells were starting to differentiate.

To examine whether dividing cells differentiate and give rise to new neuronal cells in the adult retina we double-labeled sections from BrdU-injected animals with the neuronal markers β 3-tubulin and NeuN. At P8 in the wild-type retina, β 3-tubulin was weakly detected in the photoreceptor layer and strongly localized in the ganglion cell-nerve fiber layer, the inner plexiform layer, and in a proportion of cells of the inner nuclear layer (INL), whereas NeuN labeled ganglion cells and a few cells in the INL (data not shown). Using confocal microscopy, we detected BrdU-positive cells in the adult mutant retina with β 3-tubulin-labeled processes, examples are shown at 4 (Figs. 6G, 6H) and 5 (Fig. 6I–K) weeks of age. The cells expressing β 3-tubulin were disorganized in the adult mutant retina compared with the pattern of β 3-tubulin expression observed in the adult wild-type retina (Fig. 6L), with strong expression in the ganglion cell layer and the inner plexiform layer. BrdU and NeuN colabeled cells were observed, but only rarely in the mutant retina (Fig. 6M). These were less frequent than the β 3-tubulin-positive cells, which may reflect cell immaturity as NeuN is a late neuronal marker. Immunostaining with BrdU and the glial cell marker, GFAP, did not detect colocalization, which suggests that these cells were not Müller cells. We did not detect nestin, β 3-tubulin, NeuN, or GFAP localization within the CE of the mutant or the wild type (data not shown).

New Amacrine-like Cells in the Adult *Chx10*^{-/-} Retina

To determine whether the neurons generated from RPCs in the adult mutant retina express markers characteristic of retinal neurons, immunolabeling with a range of antibodies was performed on sections from retinas pulsed with BrdU in the fourth postnatal week followed by a 3-week chase period. We found BrdU-labeled cells in the adult mutant retina expressing syntaxin (Figs. 7B, 7C) and VC1.1 (Figs. 7E, 7F), markers for amacrine and horizontal cells in the wild type (Figs. 7A, 7D). We also observed BrdU-labeled cells that colabeled for CRALBP (Figs. 7H, 7I), a marker for Müller glial cells and RPE, suggesting that some of the dividing cells were adopting a nonneuronal pathway of differentiation. Codetection of BrdU with Brn3b, blue cone opsin, rhodopsin, and recoverin was not observed. Immunostaining for neuronal markers was not detected in the CE in these experiments.

To confirm double-labeling of BrdU and retinal markers, immunostaining was performed on dissociated retinal cells from BrdU injected mutant and wild-type mice after a 3-week chase period. Codetection of BrdU with VC1.1, syntaxin, or CRALBP (Fig. 8) was observed. Because of the very small size of the adult mutant retina and the small number of BrdU-labeled cells recovered per retina, the percentage of each type of double-labeled cells could not be determined.

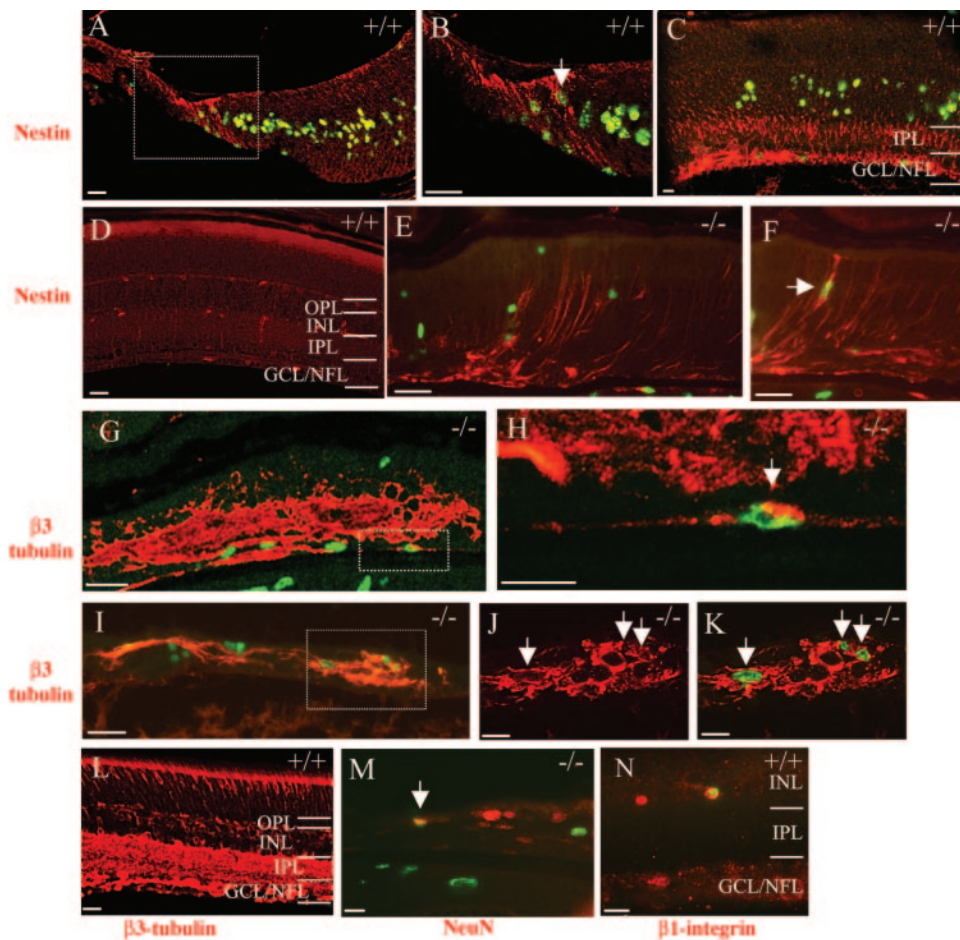


FIGURE 6. New neurons are generated in the adult mutant retina. Sections from wild-type (+/+) and mutant (-/-) eyes double labeled for BrdU (green) and nestin (A-F, red), $\beta 3$ -tubulin (G-L, red), NeuN (M, red), or $\beta 1$ -integrin (N, red). (A-C) Postnatal day 8 (P8), after a single BrdU injection on P7. BrdU labeling is observed primarily in the periphery of the wild-type retina (A, B) and decreases toward the central retina (C). Nestin-positive progenitors project radially across the retina at the periphery, and double label with BrdU (box in A magnified in B, arrow). In central retina BrdU labels late-born cells of the inner retina and colocalization of nestin and BrdU in progenitors is not detected (C). (D-H, M, N) Retinal sections at 4 weeks of age, after 2 weeks of BrdU injections. (I-L) Retinal sections at 5 weeks of age, after 2 weeks of BrdU injections. In the wild-type, BrdU-labeled cells were rarely observed, and no nestin labeling was observed (D, only autofluorescence of retinal vasculature was seen). By contrast, nestin-positive cells were observed projecting radially across the retina in the 4-week-old mutant retina (E, F) and occasionally double labeled with BrdU (F, arrow). In the mutant retina, $\beta 3$ -tubulin-labeled cells were observed at 4 (G, H) and 5 (I-K) weeks of age and revealed a relatively disorganized retinal structure; some cells labeled for both $\beta 3$ -tubulin and BrdU at each time point (indicated by arrows in H, J, and K, in confocal micrographs). By contrast, no BrdU labeling was observed in the 5-week wild-type retina, and the pattern of $\beta 3$ -tubulin labeling is more organized, with the ganglion and inner plexiform layer showing the greatest abundance (L). (M) A BrdU-labeled cell in the mutant 4-week retina colabeling with the neuronal marker NeuN (arrow). (N) A rare BrdU-labeled cell in the wild-type 4-week-old retina double labeled with $\beta 1$ -integrin, a marker for vascular endothelium. OPL, outer plexiform layer; IPL, inner plexiform layer; GCL/NFL, ganglion cell layer/nerve fiber layer; INL, inner nuclear layer. Scale bar: (A-G, I, L) 25 μ m; (H, J, K, M, N) 10 μ m.

rows in H, J, and K, in confocal micrographs). By contrast, no BrdU labeling was observed in the 5-week wild-type retina, and the pattern of $\beta 3$ -tubulin labeling is more organized, with the ganglion and inner plexiform layer showing the greatest abundance (L). (M) A BrdU-labeled cell in the mutant 4-week retina colabeling with the neuronal marker NeuN (arrow). (N) A rare BrdU-labeled cell in the wild-type 4-week-old retina double labeled with $\beta 1$ -integrin, a marker for vascular endothelium. OPL, outer plexiform layer; IPL, inner plexiform layer; GCL/NFL, ganglion cell layer/nerve fiber layer; INL, inner nuclear layer. Scale bar: (A-G, I, L) 25 μ m; (H, J, K, M, N) 10 μ m.

BrdU-Labeled Cells in the Adult Wild-Type Retinal Vasculature

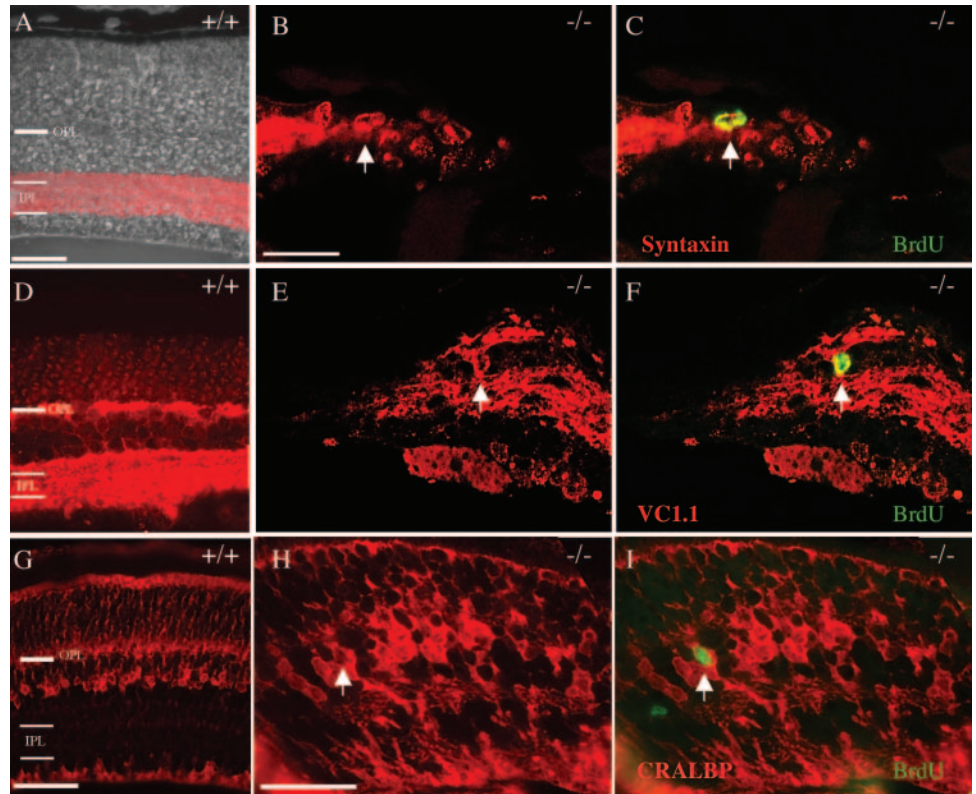
A rare population of BrdU-labeled cells, which did not label with either nestin or $\beta 3$ -tubulin, was observed in the inner layers of the adult wild-type retina (Fig. 4D). Based on their location, these cells may be part of the developing capillary plexus, which develops during the first few postnatal weeks.^{41,42} Retinal sections were immunostained for the endothelial marker, $\beta 1$ -integrin. Whereas no BrdU-labeled cells expressed $\beta 1$ -integrin in the adult mutant retina (data not shown), BrdU-labeled cell in the wild-type retina colabeled for $\beta 1$ -integrin (Fig. 6N), confirming that these cells are likely to be part of the retinal vasculature.

DISCUSSION

Our analysis of the temporal distribution of RPCs in the *Chx10*-null and wild-type retina implicates *Chx10* in regulating embryonic RPC behavior. It also shows that when *Chx10*'s function is disrupted, cells with RPC-like behavior persist in the adult retina. Of note, these RPC-like cells in the adult mutant retina are present in both central and peripheral regions. The only other examples of neurogenic progenitor-like cells present in the central retina of adult vertebrate organisms are the rod-precursor lineages of teleost fish²⁷ and Müller glial

cells in postnatal chicks.⁴³ In damaged gold fish retina, the rod-precursor cells regenerate all types of retinal neuron, whereas acute damage of the postnatal chick retina induced Müller glial cells to undergo a single round of cell division and express markers characteristic of retinal progenitors and, occasionally, retinal neurons. Similar progenitor-like cells have not been observed in mammalian retina, which does not regenerate after injury, although, in other regions of the nervous system, there is evidence that glial cells can give rise to neurons.⁴⁴ Transdifferentiation of the RPE to NR also provides a source of new neurons after retinal damage and has been shown to occur in amphibians and in chick and mammalian embryonic eyes.²⁷ That single genetic changes can result in the presence of RPC-like cells in the mature retina of mammals is a novel concept and supported by recent studies that identified persistent progenitors at the retinal margin of adult *Shh* receptor patched (*Ptc*)^{+/-} mice⁴⁵ and in the central retina of *Kip1*-null and *Kip1/p19^{INK4d}* double-null mice at P18.⁴⁶ Like *Chx10*, these genes affect proliferation of retinal progenitors, but their deficiency has different effects on the adult retina. In *Ptc*^{+/-} mice, which have constitutively activated *Shh* signaling, proliferating cells are present in the retinal margin and in the CE, and only those at the margin generated new photoreceptors in response to retinal degeneration.⁴⁵ In contrast, loss of the cyclin-dependent kinase inhibitors *Kip1* and *p19^{INK4d}*, which

FIGURE 7. Amacrine-like cells are generated in the adult mutant retina. (A–D) Sections from wild-type eyes (+/+; A, D, G) or mutant eyes injected with BrdU at P25, P27, and P29 and culled 3 weeks after the last injection (–/–; B, C, E, F, H, I) labeled for BrdU (green) and syntaxin (A–C, red), VC1.1 (D–F, red), or CRALBP (G–I). (A) Syntaxin staining imposed on a phase-contrast micrograph; staining of amacrine cells and their processes is observed at the vitreal side of the inner nuclear layer, in the inner plexiform layer (IPL) and in the ganglion cell layer adjacent to the IPL. (B, C, arrows) Cell colabeled for syntaxin and BrdU. (D) VC1.1 staining of amacrine cells in the same locations as syntaxin labeling, and also the horizontal cells on the scleral side of the inner nuclear layer and the outer plexiform layer (OPL). (E, F) Cell colabeled for VC1.1 and BrdU (arrow). (G) CRALBP staining of Müller cells in the inner nuclear layer of the retina and the RPE. (H, I, arrows) Cell colabeled for CRALBP and BrdU (arrow). Scale bar: (A, D) 100 μ m; (B, C) 45 μ m; (E, F) 55 μ m; (G, H, I) 50 μ m.



mediate exit from the cell cycle, prolongs the normal period of retinal cell proliferation and causes retinal dysplasia, including an increase in the number of horizontal cells.⁴⁶

Several important questions pertain to our findings. The first question concerns the origin of the RPC-like cells in the adult *Chx10* mutant retina. Analysis of the profile of mitotic cells during development (using H3 labeling) supports a model in which lack of *Chx10* extends the longevity of a population of embryonic RPCs. The H3 study revealed that after an early decrease in proliferation in the mutant compared with the wild-type retina, a small population of RPCs continues to proliferate steadily in the mutant. These cells are a possible source of the dividing cells observed in the adult retina. In previous studies, researchers have concluded that RPCs have a limited lifespan, as they were unable to isolate neurosphere colonies from the adult NR.²⁶ By contrast, we found that in retinas lacking *Chx10*, RPC-like cells persist into adulthood. Although we have not formally excluded a nonneuroepithelial source for the BrdU-positive cells the expression data make this unlikely. Because *Chx10* is not expressed in the RPE and BrdU-labeled cells were not observed in the RPE, migrating RPE cells are an unlikely alternative source. Moreover, a recent analysis of expression using a *Chx10*-GFP BAC reporter transgene in *Chx10*-null retina showed that in the P14 retina, GFP-positive cells expressed the Müller glial/progenitor markers CRALBP and Pax6.⁴⁷ These findings are consistent with the idea that RPC-like cells persist in the absence of *Chx10*.

Two other recent studies give new insight to our findings. Crossing the *Chx10^{orf/orf}/129/Sv* into a mixed genetic background produced a more severe phenotype, with a progressive appearance of ectopic pigmentation in the NR.⁴⁸ Labeling with the *Chx10*-GFP BAC transgene suggested that these pigment cells arose by direct transdifferentiation of NR cells. Ectopic RPE gene expression was also found in the NR from early embryonic stages suggesting that *Chx10* acts to maintain the NR by repressing expression of RPE determinants such as the *Mitf* transcription factor.^{48,49} These studies did not explore

whether the adult mutant retina contains proliferating cells. Our observation of proliferating cells in the adult retina probably reflects this instability of NR identity in the absence of *Chx10*. Nestin, VC1.1, and CRALBP immunostaining of BrdU-positive cells is consistent with a progenitor state, as these markers have been used to label neural progenitors.^{35,50} Neural retinal cells may be dividing as part of a process of transdifferentiation that involves dedifferentiation followed by proliferation and differentiation. Our data do not exclude the possibility that the dividing cells are Müller glia, although only occasional CRALBP labeling was observed, which may reflect cells' adopting an RPE fate after division. Alternatively, the dividing cells may have failed to complete normal retinal histogenesis and therefore retained progenitor characteristics into adulthood.

Do these RPC-like cells maintain neurogenic potential? We found that new neurons are being generated in the adult mutant retina, albeit in a small number and expressing only a subset of retinal neuron markers. Previous work has shown that overexpression of *Chx10* increases generation of all types of INL cells in mouse and suppressed photoreceptor development in chick, whereas lack of *Chx10* prevents bipolar cell development.^{16,51,52} That RPC-like cells in the adult mutant preferentially express INL markers (syntaxin, VC1.1) may relate to *Chx10*'s role in providing INL identity. One possibility is that progenitors that were predestined in part to produce amacrine cells selectively persisted in the mutant retina postnatally. Consistent with this idea, we found no evidence of ganglion cell, bipolar cell, or photoreceptor production. The finding that the adult mutant retina is apparently permissive for neurogenesis is surprising and suggests that the environment is not inhibitory.

Although the *Chx10*-null adult retina contains RPCs with neurogenic potential, it remains smaller than the wild type. Consistent with other studies, we found very low levels of apoptosis in the embryonic wild-type and mutant retina, and concluded that apoptosis is not likely to contribute to the cell

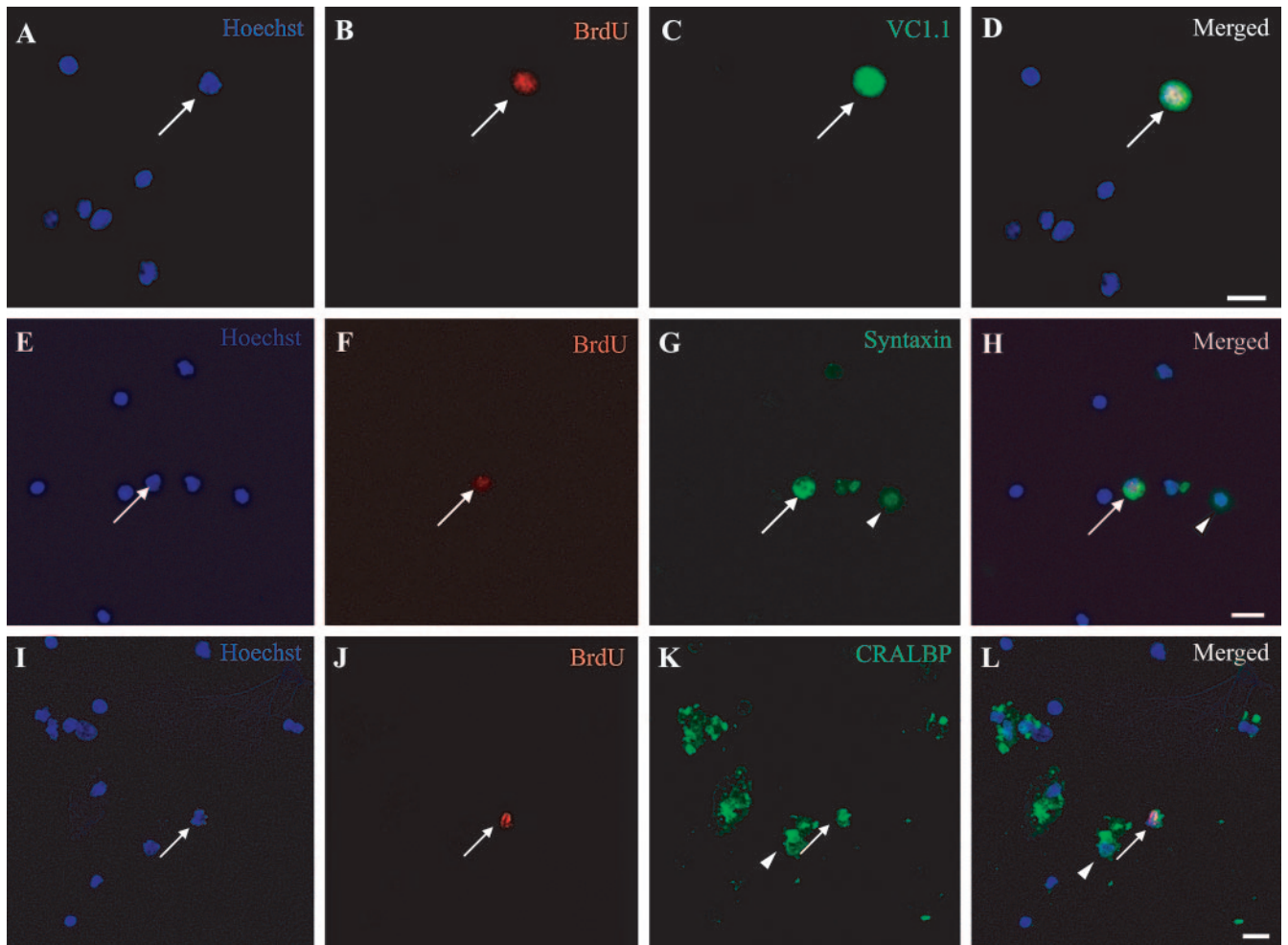


FIGURE 8. Colabeling of BrdU and retinal markers in dissociated adult *Chx10*^{-/-} retinal cells. All images show dissociated *Chx10*^{-/-} retinal cells from mice injected with BrdU at P25, P27, and P29 and culled 3 weeks after the last injection, and colabeled for BrdU (red), Hoechst nuclear dye (blue), and VC1.1 (green, A–D), syntaxin (green, E–H) or CRALBP (green, I–L). Arrows: colabeled BrdU-positive cells. Arrowheads: BrdU-negative syntaxin-positive (G–H) or BrdU-negative and CRALBP-positive (K–L) cells as the control. Scale bar, 10 μ m.

number deficit in the mutant.^{23,53–55} Rather, it is likely that the adult RPC-like cells harbor the same proliferative defects found in embryonic RPCs in the mutant and are thus unable to amplify the size of the progenitor population to drive cell number expansion and growth of the adult retina.

Properties of multipotentiality and self-renewal have been demonstrated in vitro for putative stem cells isolated from the adult CE of the rodent retina.^{25,26} In this study, we identified cycling cells in the CE of the ciliary body in the adult wild-type mouse eye in vivo. These cells are a possible source of the CE stem cells characterized in vitro. However, cycling cells were not identified at the peripheral edge of the retina (the ciliary margin). By contrast, proliferating RPCs in the ciliary margin have been identified in adult chickens,⁵⁶ quail, and opossum,⁵⁷ which show similarities with embryonic RPCs, such as expression of both *Pax6* and *Chx10*.

We identified an increased number of dividing cells in vivo within the adult CE of the mutant, compared with the wild type. Likewise, in a previous in vitro study, *Chx10* mutant CE produced more neurospheres containing fewer cells than the wild-type CE.²⁶ Both mutant and wild-type neurosphere colonies differentiated to produce neurons.²⁶ However, in vivo, the adult CE showed no evidence of neurogenesis, in contrast to the dividing cells in the mutant central retina. The different behaviors of these dividing cell populations are probably influ-

enced by differences in their extracellular environments. The relationship between the progenitor-like cells we observed in the CE and the retina, the putative retinal stem cells isolated from the CE,^{25,26} and the transdifferentiating pigment-generating cells^{48,49} have not been established and need further investigation. These findings are of interest as they suggest that manipulation of *Chx10* expression and/or extracellular factors could influence the number of cells with neurogenic potential within the mature retina.

Acknowledgments

The authors thank Jo Sinclair for technical assistance with DNA flow cytometry and Mark Hankin, Roberta Fiocco, and Patrizia Ferretti for useful discussions.

References

- Conlon I, Raff M. Size control in animal development. *Cell*. 1999; 96:235–244.
- Potten CS, Loeffler M. Stem cells: attributes, cycles, spirals, pitfalls and uncertainties: lessons for and from the crypt. *Development*. 1990;110:1001–1020.
- Hall PA, Watt FM. Stem cells: the generation and maintenance of cellular diversity. *Development*. 1989;106:619–633.

4. Alvarez-Buylla A, Lim DA. For the long run: maintaining germinal niches in the adult brain. *Neuron*. 2004;41:683-686.
5. Gage FH. Mammalian neural stem cells. *Science*. 2000;287:1433-1438.
6. Galli R, Gritti A, Bonfanti L, Vescovi AL. Neural stem cells: an overview. *Circ Res*. 2003;92:598-608.
7. Young RW. Cell differentiation in the retina of the mouse. *Anat Rec*. 1985;212:199-205.
8. Cepko CL, Austin CP, Yang X, Alexiades M, Ezzeddine D. Cell fate determination in the vertebrate retina. *Proc Natl Acad Sci USA*. 1996;93:589-595.
9. Zuber ME, Perron M, Philpott A, Bang A, Harris WA. Giant eyes in *Xenopus laevis* by overexpression of XOptx2. *Cell*. 1999;98:341-352.
10. Kobayashi M, Nishikawa K, Suzuki T, Yamamoto M. The homeobox protein Six3 interacts with the Groucho corepressor and acts as a transcriptional repressor in eye and forebrain formation. *Dev Biol*. 2001;232:315-326.
11. Lee CS, May NR, Fan CM. Transdifferentiation of the ventral retinal pigmented epithelium to neural retina in the growth arrest specific gene 1 mutant. *Dev Biol*. 2001;236:17-29.
12. Chow RL, Lang RA. Early eye development in vertebrates. *Annu Rev Cell Dev Biol*. 2001;17:255-296.
13. Fantl V, Stamp G, Andrews A, Rosewell I, Dickson C. Mice lacking cyclin D1 are small and show defects in eye and mammary gland development. *Genes Dev*. 1995;9:2364-2372.
14. Graw J. The genetic and molecular basis of congenital eye defects. *Nat Rev Genet*. 2003;4:876-888.
15. Ferda Percin E, Ploder LA, Yu JJ, et al. Human microphthalmia associated with mutations in the retinal homeobox gene CHX10. *Nat Genet*. 2000;25:397-401.
16. Burmeister M, Novak J, Liang MY, et al. Ocular retardation mouse caused by Chx10 homeobox null allele: impaired retinal progenitor proliferation and bipolar cell differentiation. *Nat Genet*. 1996;12:376-384.
17. Bar-Yosef U, Abuelaish I, Harel T, et al. CHX10 mutations cause non-syndromic microphthalmia/anophthalmia in Arab and Jewish kindreds. *Hum Genet*. 2004;115:302-309.
18. Rutherford AD, Dhomen N, Smith HK, Sowden JC. Delayed expression of the Crx gene and photoreceptor development in the Chx10-deficient retina. *Invest Ophthalmol Vis Sci*. 2004;45:375-384.
19. Liu IS, Chen JD, Ploder L, et al. Developmental expression of a novel murine homeobox gene (Chx10): evidence for roles in determination of the neuroretina and inner nuclear layer. *Neuron*. 1994;13:377-393.
20. Levine EM, Green ES. Cell-intrinsic regulators of proliferation in vertebrate retinal progenitors. *Semin Cell Dev Biol*. 2004;15:63-74.
21. Konyukhov BV, Sazhina MV. Genetic control over the duration of G1 phase. *Experientia*. 1971;27:970-971.
22. Konyukhov BV, Sazhina MV. Interaction of the genes of ocular retardation and microphthalmia in mice. *Folia Biol (Praba)*. 1966;12:116-123.
23. Green ES, Stubbs JL, Levine EM. Genetic rescue of cell number in a mouse model of microphthalmia: interactions between Chx10 and G1-phase cell cycle regulators. *Development*. 2003;130:539-552.
24. Bone-Larson C, Basu S, Radel JD, et al. Partial rescue of the ocular retardation phenotype by genetic modifiers. *J Neurobiol*. 2000;42:232-247.
25. Ahmad I, Tang L, Pham H. Identification of neural progenitors in the adult mammalian eye. *Biochem Biophys Res Commun*. 2000;270:517-521.
26. Tropepe V, Coles BL, Chiasson BJ, et al. Retinal stem cells in the adult mammalian eye. *Science*. 2000;287:2032-2036.
27. Reh TA, Levine EM. Multipotential stem cells and progenitors in the vertebrate retina. *J Neurobiol*. 1998;36:206-220.
28. Hendzel MJ, Wei Y, Mancini MA, et al. Mitosis-specific phosphorylation of histone H3 initiates primarily within pericentromeric heterochromatin during G2 and spreads in an ordered fashion coincident with mitotic chromosome condensation. *Chromosoma*. 1997;106:348-360.
29. Dyer MA, Cepko CL. Regulating proliferation during retinal development. *Nat Rev Neurosci*. 2001;2:333-342.
30. Ludbrook J. Multiple comparison procedures updated. *Clin Exp Pharmacol Physiol*. 1998;25:1032-1037.
31. Shkumatava A, Neumann CJ. Shh directs cell-cycle exit by activating p57Kip2 in the zebrafish retina. *EMBO Rep*. 2005;6:563-569.
32. Nicoletti I, Migliorati G, Pagliacci MC, Grignani F, Riccardi C. A rapid and simple method for measuring thymocyte apoptosis by propidium iodide staining and flow cytometry. *J Immunol Methods*. 1991;139:271-279.
33. Krishan A. Rapid flow cytofluorometric analysis of mammalian cell cycle by propidium iodide staining. *J Cell Biol*. 1975;66:188-193.
34. Xiang M, Zhou L, Peng YW, et al. Brn-3b: a POU domain gene expressed in a subset of retinal ganglion cells. *Neuron*. 1993;11:689-701.
35. Alexiades MR, Cepko CL. Subsets of retinal progenitors display temporally regulated and distinct biases in the fates of their progeny. *Development*. 1997;124:1119-1131.
36. Zhao Y, Hong DH, Pawlyk B, et al. The retinitis pigmentosa GTPase regulator (RPGR)-interacting protein: subserving RPGR function and participating in disk morphogenesis. *Proc Natl Acad Sci USA*. 2003;100:3965-3970.
37. Young RW. Cell proliferation during postnatal development of the retina in the mouse. *Brain Res*. 1985;353:229-239.
38. Messam CA, Hou J, Major EO. Coexpression of nestin in neural and glial cells in the developing human CNS defined by a human-specific anti-nestin antibody. *Exp Neurol*. 2000;161:585-596.
39. Ahmad I, Dooley CM, Thoreson WB, Rogers JA, Afari S. In vitro analysis of a mammalian retinal progenitor that gives rise to neurons and glia. *Brain Res*. 1999;831:1-10.
40. Insua MF, Garelli A, Rotstein NP, et al. Cell cycle regulation in retinal progenitors by glia-derived neurotrophic factor and docosahexaenoic acid. *Invest Ophthalmol Vis Sci*. 2003;44:2235-2244.
41. Feeney SA, Simpson DA, Gardiner TA, et al. Role of vascular endothelial growth factor and placental growth factors during retinal vascular development and hyaloid regression. *Invest Ophthalmol Vis Sci*. 2003;44:839-847.
42. Friedlander M, Theesfeld CL, Sugita M, et al. Involvement of integrins alpha v beta 3 and alpha v beta 5 in ocular neovascular diseases. *Proc Natl Acad Sci USA*. 1996;93:9764-9769.
43. Fischer AJ, Reh TA. Muller glia are a potential source of neural regeneration in the postnatal chicken retina. *Nat Neurosci*. 2001;4:247-252.
44. Doetsch F, Caille I, Lim DA, Garcia-Verdugo JM, Alvarez-Buylla A. Subventricular zone astrocytes are neural stem cells in the adult mammalian brain. *Cell*. 1999;97:703-716.
45. Moshiri A, Reh TA. Persistent progenitors at the retinal margin of ptc+/- mice. *J Neurosci*. 2004;24:229-237.
46. Cunningham JJ, Levine EM, Zindy F, et al. The cyclin-dependent kinase inhibitors p19(Ink4d) and p27(Kip1) are coexpressed in select retinal cells and act cooperatively to control cell cycle exit. *Mol Cell Neurosci*. 2002;19:359-374.
47. Rowan S, Cepko CL. Genetic analysis of the homeodomain transcription factor Chx10 in the retina using a novel multifunctional BAC transgenic mouse reporter. *Dev Biol*. 2004;271:388-402.
48. Rowan S, Chen CM, Young TL, Fisher DE, Cepko CL. Transdifferentiation of the retina into pigmented cells in ocular retardation mice defines a new function of the homeodomain gene Chx10. *Development*. 2004;131:5139-5152.
49. Horsford DJ, Nguyen MT, Sellar GC, et al. Chx10 repression of Mitf is required for the maintenance of mammalian neuroretinal identity. *Development*. 2005;132:177-187.
50. Walcott JC, Provis JM. Muller cells express the neuronal progenitor cell marker nestin in both differentiated and undifferentiated human foetal retina. *Clin Exp Ophthalmol*. 2003;31:246-249.

51. Hatakeyama J, Tomita K, Inoue T, Kageyama R. Roles of homeobox and bHLH genes in specification of a retinal cell type. *Development*. 2001;128:1313-1322.
52. Toy J, Norton JS, Jibodh SR, Adler R. Effects of homeobox genes on the differentiation of photoreceptor and nonphotoreceptor neurons. *Invest Ophthalmol Vis Sci*. 2002;43:3522-3529.
53. Pequignot MO, Provost AC, Salle S, et al. Major role of BAX in apoptosis during retinal development and in establishment of a functional postnatal retina. *Dev Dyn*. 2003;228:231-238.
54. Robb RM, Silver J, Sullivan RT. Ocular retardation (or) in the mouse. *Invest Ophthalmol Vis Sci*. 1978;17:468-473.
55. Silver J, Robb RM. Studies on the development of the eye cup and optic nerve in normal mice and in mutants with congenital optic nerve aplasia. *Dev Biol*. 1979;68:175-190.
56. Fischer AJ, Reh TA. Identification of a proliferating marginal zone of retinal progenitors in postnatal chickens. *Dev Biol*. 2000;220:197-210.
57. Kubota R, Hokoc JN, Moshiri A, McGuire C, Reh TA. A comparative study of neurogenesis in the retinal ciliary marginal zone of homeothermic vertebrates. *Brain Res Dev Brain Res*. 2002;134:31-41.